Calcium Binding and Homoassociation of E-cadherin Domains†

Alexander W. Koch, Sabine Pokutta,‡ Ariel Lustig, and Jürgen Engel*

Department of Biophysical Chemistry, Biozentrum, University of Basel, Klingelbergstrasse 70, 4056 Basel, Switzerland

Received March 12, 1997; Revised Manuscript Received May 1, 1997⊗

ABSTRACT: Cadherins are single pass transmembrane glycoproteins which mediate calcium dependent cell−cell adhesion by homophilic interactions. To reveal the molecular details of calcium binding and homoassociation, we recombinantly expressed in *Escherichia coli* a domain pair consisting of the first two domains of E-cadherin (ECAD12) and the single domains 1, 2, and 5. ECAD12 encompasses the most N-terminal of the four putative calcium-binding pockets in the extracellular region of E-cadherin. Equilibrium dialysis experiments revealed that the single domains do not bind Ca^{2+}, but ECAD12 was found to bind three calcium ions. ECAD12 dimerizes ($K_d = 0.08 \pm 0.02$ mM) in the presence of Ca^{2+} as we could demonstrate by analytical ultracentrifugation. Calcium binding to ECAD12 induces conformational changes which were monitored by electrophoretic mobility and by circular dichroism. By analyzing our equilibrium dialysis data with a single binding site model, we found an average K_d of 460 μM for the three bound Ca^{2+}. Assuming a model for three binding sites, which slightly increased the quality of the fit, we obtained two identical K_ds of 330 μM and a third much higher K_d of 2 mM. The entire extracellular region of E-cadherin, which was recombinantly expressed in mammalian cells, binds nine Ca^{2+} with a much lower average K_d of 30 μM. Therefore, we conclude that the four calcium binding pockets are not identical. Since binding to ECAD12 occurs at Ca^{2+} concentrations close to those in the extracellular space, we suggest that the N-terminal domain pair might be involved in calcium regulation of E-cadherin mediated cell−cell adhesion.

E-cadherin is a 120 kD transmembrane glycoprotein and belongs, like N-, P-, R-, B-cadherin, and L-CAM, to the classical cadherins which represent a subclass of the large and diverse cadherin superfamily (*1*). Classical cadherins consist of five extracellular cadherin repeats with approximately 110 amino acids each, a transmembrane part, and a highly conserved cytosolic domain which connects them to the actin cytoskeleton via the catenins (*2*). The cadherin repeats are defined by their internal homology and by the presence of putative calcium-binding motifs at conserved positions (*1*, *3*). Cadherins are mediators of Ca^{2+}-dependent cell−cell adhesion and are essential in initiation, maintenance, and proper functioning of tissue architecture (*4*). Since multiple cadherins differ in their expression patterns and dynamic changes occur in cell adhesion, cadherins are thought to be important regulators of animal morphogenesis (*3*, *5*).

One hallmark of the cadherin-mediated cell−cell adhesion is the homotypic mode of interaction of these cell adhesion molecules (*3*). Nevertheless, more and more examples for heterophilic interactions were reported such as the interaction between different cadherins or between E-cadherin and αEβ7/αM290β7 (*6*, *7*), an integrin of the T-lymphocyte adhesion system. Structural data available now for N-terminal cadherin fragments (*8*−*10*) suggest molecular details of cadherin self-association. Both homophilic and heterophilic interactions require high local concentration of cadherin molecules as present on the cell surface (*7*) and as it can be mimicked by the artificially clustered ECAD-COMP (*11*).

The second hallmark of the cadherin mediated cell−cell adhesion is the Ca^{2+} dependence of this process. It has been demonstrated that cadherins exhibit their adhesive function only in the presence of Ca^{2+} and that they are degraded by proteases in the absence of Ca^{2+} (*2*). Calcium binding to E-cadherin has been shown by Western Blot experiments (*12*), and the importance of the calcium-binding site between domains 1 and 2 has been demonstrated by a point mutation which abolished the adhesive function of the protein (*13*). The finding that 50% of diffuse-type gastric carcinomas, which all show diminished cell−cell adhesion, contain mutations in the E-cadherin gene resulting in alterations of putative calcium-binding sites furthermore stresses the importance of calcium binding for proper functioning of E-cadherin (*14*).

Structural changes of the extracellular region of E-cadherin upon calcium binding has been confirmed by electron microscopy and spectroscopic methods (*15*). Electron microscopy demonstrated that the extracellular part of E-cadherin undergoes a reversible conformational change from a rod-like structure to a more condensed structure upon Ca^{2+} depletion. High resolution structure determinations of N-terminal domains of N- and E-cadherin revealed that calcium-binding sites reside in the interface of two consecutive cadherin domains (*8*, *9*). Recently, the X-ray structure of a recombinant fragment consisting of the first two E-cadherin domains elucidated how three calcium ions are complexed between these two domains (*10*). Thirteen amino acid residues and, in addition, two water molecules coordinate three calcium ions leading to a complex network of interactions. Calcium ions bridge between the domains and

† This work was supported by funds from the Swiss National Science Foundation (Grant 3-32251.91).

* To whom correspondence should be addressed. Tel: +41-61-2672250. Fax: +41-61-2672289.

‡ Present address: Department of Structural Biology, Fairchild Building, Stanford University, School of Medicine, Stanford, CA 94305.

⊗ Abstract published in *Advance ACS Abstracts,* June 15, 1997.

S0006-2960(97)00562-X CCC: $14.00

induce conformational changes within the proposed homophilic binding surface (*8*). This may explain the rigidification of the extracellular part of E-cadherin and the calcium dependence of adhesion.

Cadherin mediated cell−cell adhesion is regulated by calcium binding, but in earlier studies (*15*, *16*), only average K_d values for calcium binding to E-cadherin were determined by indirect methods. The aim of the present work was to evaluate mechanisms of calcium induced regulation by direct measurement of calcium binding to individual domains and by measuring calcium-dependent homoassociation. Since N-terminal fragments are crucial for the adhesive function of cadherins (*11*, *17*), we recombinantly expressed a domain pair consisting of the first two N-terminal domains of E-cadherin and, in addition, the single domains 1, 2, and 5. Calcium binding was only found for the domain pair, and calcium-dependent homoassociation was measured by analytical ultracentrifugation. Binding data were evaluated for the domain pair and for the entire extracellular part of E-cadherin by equilibrium dialysis. Our data were compared with the recently solved X-ray structure of an E-cadherin fragment very similar to our domain pair (*10*).

EXPERIMENTAL PROCEDURES

Plasmid Reconstructions. The cDNA of mouse E-cadherin (*18*) was kindly provided by Dr. J. Stappert, Max-Planck-Institut für Immunbiologie, Freiburg im Breisgau, Germany. The cDNA was used as a template for PCR amplification of DNA fragments coding for the first two domains, designated as ECAD12, and coding for single domains, designated as ECAD1, ECAD2, and ECAD5. The decision on domain boundaries was guided by the assignment of repeats in the E-cadherin sequence obtained from SwissProt Data Base (CADEmouse, AC P09803).

For ECAD12, a DNA fragment coding for residue 157−375 was generated by the use of a 5′ primer introducing a *Nde*I site and a start codon (5′ end, CCC CAT ATG GAC TGG GTC ATC CCT C) and a 3′ primer introducing two arginines as a trypsin cleavage site and a *Xho*I site (3′ end, CCC CTC GAG ACG ACG AGG AGC GTT GTC ATT AAT A). For ECAD2, a DNA fragment coding for residues 264 to 375 was generated by using a 5′ primer with a *Nde*I site and a start codon (5′ end, CCC CAT ATG TTT ACC CAG GAG GTG TTT) and the 3′ primer of ECAD12. ECAD1-DNA coding for residues 157−262 was constructed using a 5′ primer including a *Nde*I site and a 3′ primer including a *Hin*dIII site and a stop codon (5′ end, CCC CAT ATG GAC TGG GTC ATC C; 3′ end, CCC AAG CTT TTA TGG CCT GTT GTC ATT CTG). ECAD5-DNA coding for residues 596−709 was constructed using a 5′ primer including a *Nde*I site and a 3′ primer including a *Eco*RI site and a stop codon (5′ end, CCC CAT ATG ATC CCA GAA CCT CG; 3′ end, CCC GAA TTC TTA AAC TTG CAA TCC TGC TG). The amplified products of ECAD12 and ECAD2 were cloned into a pET-22b expression vector (Novagen) using a *Nde*I/*Xho*I site. The vector encodes a C-terminal peptide LGHHHHHH which serves as affinity tag for the later purification on a metal chelating column. The amplified products of ECAD1 and ECAD5 were cloned into a pET-15b vector (Novagen) using *Nde*I/*Hin*dIII and *Nde*I/*Eco*RI sites, respectively. This vector encodes an N-terminal peptide MGSSHHHHHHSSGLVPRGS, containing a stretch of six histidines followed by a thrombin recognition site.

PCR[1] amplification of the fragments, digestion with restriction enzymes, ligation of the fragments into the appropriate vectors, and subsequent transformation into host strains were all done according to standard protocols, utilizing *Pfu* polymerase (Stratagene), restriction enzymes, and T4 DNA ligase from Boehringer Mannheim Inc. Recombinant plasmid DNA was purified from *Escherichia coli* JM109 (DE3) host strain (Promega) using a QIAspin plasmid kit (Qiagen). All amplified products were sequenced by the dideoxy chain termination method (*19*) using vector-derived primers.

Expression, Purification, and Protease Cleavage. The recombinant E-cadherin fragments were expressed in *E. coli* BL21(DE3) strain (Novagen), which contains a chromosomal copy of the T7 RNA polymerase gene under the control of lacUV5 promotor (*20*). LB media cultures of 250 mL containing 100 μg/mL ampicillin were inoculated either by freshly transformed colonies picked from agar plates or by 2 mL starting cultures which were inoculated themselves from a glycerol stock. Cultures were grown at 37 °C until an optical density $OD_{600} = 0.8-1.0$ was reached. Expression was induced by the addition of 1 mM IPTG, and the bacteria were incubated for another 3−4 h. Cells were harvested by centrifugation at 5000*g* for 10 min and stored at −70 °C.

In the case of ECAD12 and ECAD2, cell pellets were resuspended in lysis buffer (50 mM Tris, pH 8.0, 0.1% Triton) followed by addition of lysozyme (final concentration, 0.1 mg/mL) and were incubated for 30 min at room temperature. In the case of ECAD1 and ECAD5, cell pellets were resuspended in binding buffer (20 mM Tris/HCl, pH 7.9, 500 mM NaCl, 5 mM imidazole) of 4 °C containing 6 M urea as these fragments were mainly found in inclusion bodies and were purified applying denaturing conditions. Resuspended bacterial cell pellets were lysed by sonification, and the cell debris was removed by centrifugation (13000*g* for 20 min). After filtration of the supernatant through a 0.45 μm filter and dialysis against binding buffer, the crude cell extracts were applied to an affinity column. The purification using Nickel sepharose chromatography (Novagen) was performed either under denaturing (ECAD1 and ECAD5) or under native conditions (ECAD12 and ECAD2) according to the manufacturer's instructions (Novagen).

Recombinant fragments cloned in the pET-22b vector (ECAD12 and ECAD2) were expressed with a C-terminal histidine tag and a trypsin cleavage site. The histidine tag could be cleaved off by digestion with trypsin using 5 units of enzyme/μmol of protein. Digestion was complete after 5−10 min incubation at room temperature in trypsin cleavage buffer (Tris/HCl, pH 7.4, 150 mM NaCl). Immediately after digestion, trypsin was inactivated by the addition of α_2-macroglobulin (*21*). The recombinant fragments ECAD1 and ECAD5 were expressed with an N-terminal histidine tag which was cleaved off by thrombin (Sigma). Thrombin digestion was carried out in 2 M urea using 5 units of

[1] Abbreviations: PCR, polymerase chain reaction; IPTG, isopropyl-1-β,D-thiogalactopyranoside; SDS−PAGE, sodium dodecyl sulfate−polyacrylamide gel electrophoresis; FPLC, fast-performance liquid chromatography; DTT, 1,4-dithio-D,L-threitol; TBS, Tris-buffered saline; CD, circular dichroism; Fluo-3, 1-[2-amino-5-(2,7-dichloro-6-hydroxy-3-oxy-9-xanthenyl)-phenoxy]-2-[2-amino-5-methylphenoxy]ethane-*N*,*N*,*N*′,*N*′-tetraacetic acid.

thrombin/mg of protein and incubating at room temperature for 5 h in thrombin cleavage buffer (20 mM Tris/HCl, pH 8.4, 150 mM NaCl, 2.5 mM $CaCl_2$). Thrombin was inactivated by lowering the pH. Time dependence of the protease cleavage was monitored by Tricine SDS−PAGE (*22*). After adjusting pH to 7.4 and ionic strength to 500 mM NaCl, all cleaved fragments were applied a second time to the Nickel sepharose column. Uncleaved material, the histidine peptides, and *E. coli* proteins with affinity to the histidine binding column were retained on the column whereas the cleaved fragments were recovered in the flow-through. Also, trypsin bound to α_2-macroglobulin was separated from the cleaved protein by the second Nickel sepharose column run. ECAD12 was further purified by FPLC using a Superose 12 gel filtration column (Pharmacia). Purity of the proteins was judged by SDS-gel electrophoresis and Coomassie Blue staining. Protein concentrations were determined spectrophotometrically by absorbance measurements at 280 nm. The absorbance coefficients were evaluated on the basis of the amino acid composition using a molar absorption coefficient of 5540 M^{-1} cm^{-1} for tryptophan residues and 1480 M^{-1} cm^{-1} for tyrosine residues (*23*). N-terminal sequencing and dansylchloride amino acid analysis was performed by Dr. Paul Jenö (Biozentrum, Universität Basel).

The extracellular region of E-cadherin, designated as 84 kD fragment, was expressed in human embryonal kidney 293 cells, and the secreted protein was purified from serum free culture medium by DEAE-cellulose and Superose 12 column chromatography (*11*).

Gel Electrophoresis. Proteins were analyzed by SDS−PAGE as described by Laemmli (*24*) and by Tricine SDS−PAGE (*22*) using 12 × 13 cm slab gels. Protein bands were visualized by Coomassie Blue staining and molar masses were estimated by comparing bands with low molar mass standards (Pharmacia, range 94−14.4 kD). Nondenaturing PAGE was performed in a Mini-PROTEAN II apparatus (Bio-Rad) using 15% acrylamide gels and 0.92 M Tris/HCl, pH 8.8, as sample buffer (*25*).

Protein Refolding and Redox Shuffling. The cysteine containing fragments ECAD1 and ECAD5, purified under denaturing conditions, were reduced by adding DTT, subsequently reoxidized, and renatured in the presence of a redox shuffling system according to Jaenicke and Rudolph (*26*). Thrombin digested and purified samples containing 2 M urea were reduced in TBS buffer (pH 8.5, 3 mM EDTA) by adding 10 mM DTT and incubating for 2 h at room temperature. The reduced samples were rapidly diluted to 20−50 fold in refolding buffer (100 mM Tris/HCl, pH 7.4, 1 mM EDTA, 0.3 mM glutathione disulfide, 3 mM reduced glutathione), resulting in a final protein concentration of 10−50 μg/mL and an urea concentration below 0.1 M. The solution was stirred for 24 h at room temperature. Refolding was evaluated by CD spectroscopy and trypsin stability.

Partly disulfide linked ECAD12 samples were analyzed by redox-shuffling. Reduced protein samples were subsequently reoxidized in the presence of a thiol/disulfide redox pair, which serves as a shuffling reagent. Samples were reduced by incubation with 100 mM DTT at 37 °C for 30 min. The protein was salt precipitated (75% ammonium sulfate) and resuspended in redox-shuffling buffer (200 mM NaCl, 200 mM Tris/HCl, pH 8.5, 2 mM $CaCl_2$) containing 10 mM oxidized and 1 mM reduced glutathione. The mixture was incubated for 24 h, and the reoxidation process was monitored by nondenaturing PAGE. Correct folding of the protein after the reoxidation procedure was judged by CD spectroscopy.

Analytical Ultracentrifugation. To analyze the recombinant fragments by analytical ultracentrifugation, sedimentation velocity and sedimentation equilibrium experiments were performed in a Beckmann XLA analytical ultracentrifuge in 4 mm home-made double sector cells with a filling height of 1.5 mm. The ultracentrifuge was equipped with absorption optics, and an AN-60Ti rotor was used. Sedimentation coefficients were evaluated from sedimentation velocity experiments at rotor speeds of 56 000 rpm and corrected to water under standard conditions (*27*). Sedimentation equilibrium runs were performed with a rotor velocity of 20 000 rpm at 20 °C. Molar masses were determined from ln A versus r^2 plots, where A is the absorbance and r is the distance from the rotor center (*28*). A floating base line computer program was used that adjusts the base line absorbance to obtain the best linear fit of ln A versus r^2. For all cases, the partial specific volume was assumed to be 0.73 mL/g and the buffer density was taken from handbooks. Recombinant fragments were dissolved in TBS buffer (20 mM Tris/HCl, pH 7.4, 150 mM NaCl) containing 2 mM $CaCl_2$ or were Ca^{2+} depleted. Protein concentrations used here were 0.1−0.5 mg/mL (0.004−0.02 mM for ECAD12).

In order to analyze self-association of ECAD12, sedimentation equilibrium experiments were performed with two modes according to two different concentration ranges. For the concentration range of 2−11 mg/mL (0.08−0.46 mM) the Yphantis short column method was used (*29*). Equilibrium experiments were performed in a Beckmann (model E) analytical ultracentrifuge equipped with Schlieren optics at a rotor speed of 16 000 rpm at 20 °C. Molar masses were determined according to Yphantis (*29*). For the concentration range 0.5−3 mg/mL (0.02−0.12 mM), sedimentation equilibrium runs were carried out in a Beckmann XLA analytical ultracentrifuge equipped with absorption optics as described above. Experiments were carried out either in the presence of DTT or under oxidizing conditions but after removal of disulfide linked dimers via gel filtration.

Weight Average Molar Mass and Self-Association. A monomer−dimer equilibrium was assumed with the equilibrium dissociation constant

$$K_d = \frac{{c_1}^2}{c_2} \tag{1}$$

Molar concentration of monomers and dimers are c_1 and c_2, respectively, and the total molar concentration of the monomers is

$$c_0 = c_1 + 2c_2 \tag{2}$$

For self-associating systems, apparent molar masses can be determined from sedimentation equilibrium experiments. The apparent weight average molar mass ($M_{W,app}$) is related to the true average molar mass (M_W) by

$$\frac{1}{M_{W,app}} = \frac{1}{M_W} + BM_1c_0 \tag{3}$$

where B is an apparent virial coefficient and M_1 the molar

mass of the monomer (*30*). M_w is defined by

$$M_w = \frac{c_1 M_1^2 + c_2 M_2^2}{c_1 M_1 + c_2 M_2} \quad (4)$$

and it follows with the molar mass of the dimer $M_2 = 2M_1$ and eq 3

$$\frac{1}{M_{W,app}} = \frac{c_1 + 2c_2}{c_1 + 4c_2}\frac{1}{M_1} + BM_1c_0 \quad (5)$$

from eqs 1 and 2 the concentrations of the monomers c_1 and the dimers c_2 can be calculated by

$$c_1 = c_0 - 2c_2 = \frac{-1 + \sqrt{1 + 8c_0/K_d}}{4/K_d} \quad (6)$$

Dissociation constants were determined by fitting eqs 5 with 6 to the experimental concentration dependence of the apparent molar masses using a nonlinear least-square fit procedure (Sigma Plot, Jandel Sci. Corp.).

Removal of Bivalent Cations and Determination of Contaminating Ca^{2+}. Ca^{2+} ions were removed from buffers and protein solutions by passing them over an EDTA-agarose column (*31*). Remaining levels of Ca^{2+} ions were determined by using the fluorescent dye Fluo-3 (Molecular Probes Inc.), and the fluorescence was measured with a Jasco FP-777 (Jasco Co., Tokyo) spectrophotometer. The amount of Ca^{2+} ions was calculated according to Eberhard and Erne (*31*).

CD Measurements. CD measurements were performed with a Jasco J 720 spectropolarimeter (Jasco Co., Tokyo). Spectra were recorded at 20 °C in a quartz cell with a path length of 2 mm at protein concentrations ranging from 4 to 16 μM in 20 mM Tris/HCl, pH 7.4. Protein concentrations obtained from absorbance measurements at 280 nm were used to calculate the mean molar residue ellipticity (expressed in degrees squared centimeters per decimole). Spectroscopic titrations were performed at a protein concentration of 6 μM by adding aliquots of Ca^{2+} stock solutions to the Ca^{2+} depleted protein. The relative change of the mean molar residue ellipticity at four different wavelengths (210, 215, 220, and 230 nm) was calculated, and the titration data were analyzed as described earlier (*15*). The Hill equation was fitted to the experimental data with the computer program CURVFIT 1.0 (Technosoft, Graz) by using a Marquart nonlinear least-squares fit procedure.

Equilibrium Dialysis Experiments. Calcium binding was determined by equilibrium dialysis using a microdialysis system (*32*). Equilibrium dialysis experiments were performed as earlier described (*33*) with slight differences summarized here.

Aliquots of 150 μL of Ca^{2+}-depleted protein samples in standard buffer (20 mM Tris/HCl, pH 7.4, 150 mM NaCl) were dialyzed against the same volume of standard buffer containing $^{45}Ca^{2+}$ (0.1 μCi/mL) and varying concentrations of unlabeled Ca^{2+} (up to 5 mM). Protein concentrations used in the equilibrium dialysis varied from 10 to 250 μM depending on the Ca^{2+} concentration. After dialyzing the samples for 18 h at 23 °C, 100 μL aliquots were removed from each chamber and the radioactivity was determined in a liquid scintillation spectrometer. From the measured radioactivity, the moles of bound calcium per mole of protein and the free calcium concentration were determined. The protein concentrations in these experiments were ranging from 10 to 250 μM. High protein concentrations are necessary to obtain reliable values at high total Ca^{2+} concentrations.

The binding data were analyzed using a theoretical model of ligand binding to one class of calcium-binding sites (i = 1) or to multiple classes of binding sites. The moles of bound Ca^{2+} per mole of protein was calculated according to

$$B = \sum_i \frac{n_i[Ca^{2+}]/K_{d_i}}{1 + [Ca^{2+}]/K_{d_i}} \quad (7)$$

where n is number of calcium-binding sites of each class, K_{d_i} is the dissociation constant of the ith class and $[Ca^{2+}]$ is the free Ca^{2+} concentration. The models were fitted to the experimental data using nonlinear least-squares fit procedures with the computer program CURVFIT 1.0 (Technosoft, Graz). The 95% confidence limit of X^2 and R_{xy} values higher than 0.95 were used as criteria for the goodness of the fit.

RESULTS

Expression and Purification. With the aim of obtaining sufficient amounts for biophysical and biochemical studies, different E-cadherin fragments were overexpressed in *E. coli*. This work is mainly focused on ECAD12, a domain pair consisting of the first two N-terminal domains of murine E-cadherin, but also single domain fragments, namely ECAD1, ECAD2, and ECAD5, were under investigation. In addition, the entire extracellular part of E-cadherin (84 kD fragment), recombinantly expressed in a mammalian cell line (*11*), was studied.

The domain pair and the single domain fragments were designed according to the proposed domain organization (SwissProt Data Base) using PCR amplifications. The C-terminal boundaries of domain one and two were assessed due to the sequence alignment of Overduin et al. (*8*). ECAD12 starts with residue aspartate 157, since in biosynthesis E-cadherin is expressed with a propeptide which is cleaved off after arginine 156 by an endogenous protease (*11*, *34*) and ends at proline 375. ECAD12, therefore, includes all putative calcium-binding motifs in the interface of domain one and two (*8*). The construct also contains a foreign methionine at the N-terminus as a start signal and a foreign arginine after trypsin cleavage at the C-terminus (see below). ECAD2 was constructed in the same way starting with a methionine at position 262 instead of a glutamic acid. Notably, this glutamic acid is not conserved among the different E-cadherin domains. ECAD2 possesses the same C-terminus as ECAD12. ECAD1 and ECAD5 were constructed with N-terminal histidine tags followed by thrombin cleavage sites.

The histidine tagged ECAD12 was overexpressed in *E. coli* and purified using Nickel sepharose chromatography (Figure 1). The histidine tag could be cleaved off efficiently by trypsin in the presence of 2 mM Ca^{2+}. Trypsin was inactivated by binding to α_2-macroglobulin. This was judged by the absence of any trypsin activity after adding α_2-macroglobulin. The cleaved protein was then recovered in the flow-through after a second Nickel affinity column run

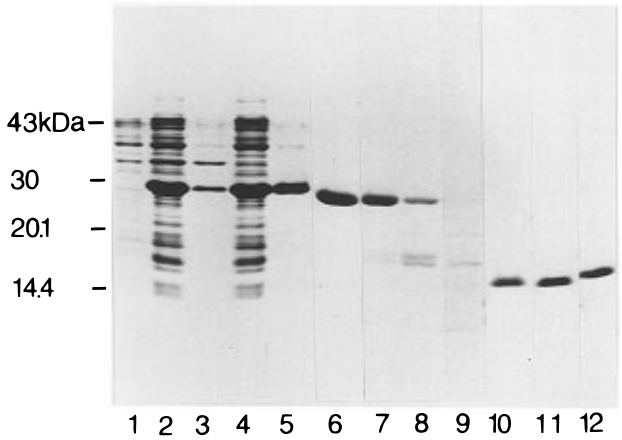

FIGURE 1: Expression, purification, and trypsin digestion of ECAD12 analyzed on Tricine SDS−PAGE. Bacterial extracts (lane 1, before induction; lane 2, after 3 h induction) were purified on a nickel sepharose affinity column. Lane 3 shows the insoluble fraction of the bacterial extract and lane 4 the soluble fraction which was passed over the column. The protein was recovered in the elute fraction (lane 5) and the histidine tag was cleaved off by a short incubation with trypsin (lane 6, 10 min digestion). To test protein stability, ECAD12 was trypsin digested for 30 min in the presence (lane 7) or absence of Ca^{2+} (lane 8, 5 mM EDTA) or digested after heat denaturation (lane 9). Lanes 10, 11, and 12 are showing the purified single domain fragments ECAD1, ECAD2, and ECAD5.

and separated from uncleaved protein, *E. coli* proteins with affinity to the Nickel sepharose resin, and most of α_2-macroglobulin with bound trypsin on it. Finally, the protein was purified to homogeneity by gel filtration chromatography on a Superose 12 column (Figure 1, lane 6). The correct N-terminus of the fragment and the complete removal of the histidine tag was revealed by N-terminal sequencing and amino acid analysis (not shown). The domain pair itself is stable against trypsin digestion in the presence of 2 mM Ca^{2+}. Only a minor part is cleaved into smaller fragments (Figure 1, lane 7). The small amounts of degradation products were thoroughly separated from ECAD12 by gel-filtration chromatography on Superose 12 (not shown). In the absence of Ca^{2+} (5 mM EDTA), ECAD12 is cleaved to much larger extent and the heat denatured protein is completely degraded by trypsin (Figure 1, lanes 8 and 9). The trypsin digestion described here enabled us to remove the histidine tag and to prove the proper folding of ECAD12 in one step since possible trypsin cleavage sites are only buried in the folded protein.

ECAD2 was purified, and the C-terminal histidine tag was cleaved off by trypsin as outlined for ECAD12. ECAD1 and ECAD5 were recovered in inclusion bodies during expression in *E. coli*, but could be purified and thrombin digested under partly denaturing conditions (2 M urea) and subsequently refolded using a renaturation protocol (see Experimental Procedures). Complete removal of C- or N-terminal histidine tags was evaluated by amino acid analysis or N-terminal sequencing. For all fragments, the correct folding was evaluated by CD spectroscopy and trypsin stability. CD spectroscopy can be used here as a criterion for proper folding since the spectra of our recombinant fragments revealed to be very similar to the CD spectrum of the 84 kD fragment (*15*).

Nondenaturing Gel Electrophoresis and Analytical Ultracentrifugation at Low Protein Concentrations. Self-association of recombinant fragments ECAD12, ECAD1, and

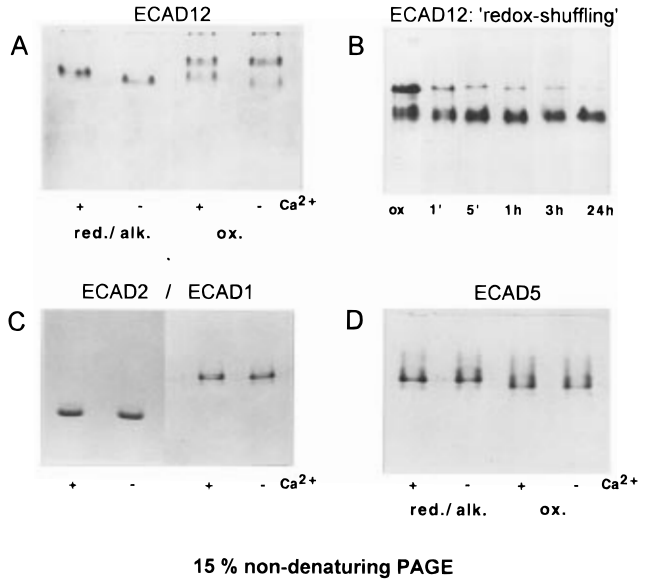

FIGURE 2: Nondenaturating gel electrophoresis of E-cadherin fragments ECAD12, ECAD2, and ECAD5. (A) Under oxidizing conditions ECAD12 partly forms dimers in solution (lanes 3, and 4). After reduction and alkylation, the protein reveals to be completely monomeric (lanes 1, and 2). In all cases, the electrophoretic mobility was smaller in the presence of 2 mM Ca^{2+} than in the presence of 5 mM EDTA. (B) The mixed populations of monomer and dimer (lane 1) could be transformed in a solely monomeric population via reducing and subsequent reoxidation by redox shuffling for 1 min to 24 h with a mixture of oxidized and reduced glutathione. (C) ECAD1 and ECAD2 do not show any significant change in their electrophoretic mobilities upon the addition of Ca^{2+}. (D) The reduced mobility upon reduction and alkylation for ECAD5 (lanes 1 and 2) compared to its oxidized form (lanes 3 and 4) indicates formation of intramolecular disulfide bonds for this fragment.

ECAD5 was studied by nondenaturing gel electrophoresis, which separates proteins on the basis of a combination of molar mass and net charge.

A slow migrating band (Figure 2A) indicated a fraction of dimers under oxidizing conditions for ECAD12. Dimers completely disappeared after reduction and subsequent alkylation of the protein demonstrating that they are not stabilized by noncovalent interactions at a protein concentration of 0.5 mg/mL as used in these experiments. These findings were supported by the molar masses obtained from analytical ultracentrifugation experiments. Sedimentation equilibrium centrifugation in the presence of DTT and at a protein concentration of 0.5 mg/mL revealed a single population for ECAD12 with a molar mass similar to the theoretical calculated molar mass of 24 kD for the monomer (Table 1). In the absence of reducing reagents a mixture of two populations with molar masses of the monomer and the dimer were observed (Table 1).

Formation of disulfide linked dimers was never complete, and variable fractions were obtained from different preparations of ECAD12. Redox shuffling did not increase the dimer fraction, but led to complete monomerization (Figure 2B). Therefore, we conclude that the monomeric form is the thermodynamic stable form of ECAD12. Disulfide-linked dimers and monomers were separated by gel filtration chromatography (data not shown). These results clearly demonstrate that ECAD12 is able to form disulfide-linked dimers under oxidizing conditions, which represent an accidental chemical cross-linking due to air oxidation during

Table 1: Molar Masses and Sedimentation Coefficients of Recombinant Fragments Determined by Analytical Ultracentrifugation[a]

fragment		s_{20w} [S][a]	M_r [kD][b]
ECAD1−2	reduced/+Ca	2.2	24.4
	reduced/−Ca	2.2	24.5
	oxidized/+Ca	3.4	23.8/47.0
	oxidized/−Ca	3.1	22.0/48.0
ECAD5	reduced/+Ca	1.6	11
	oxidized/+Ca	1.4	16
	oxidized/−Ca	1.5	14
ECAD1	oxidized/+Ca	1.5	12.3

[a] The sedimentation coefficients of 1.5 for a single domain, 2.2 for the domain pair under reducing and 3.1 to 3.3 under nonreducing conditions also suggest a dimer formation for ECAD12 under nonreducing conditions. [b] Molar masses determined by analytical ultracentrifugation revealed that ECAD12 (theoretical molar mass, 24 kD) is monomeric under reducing conditions and partly forms dimers under nonreducing conditions. The molar masses determined for ECAD5 and ECAD1 (theoretical molar masses, 13 and 12 kD) indicate no dimer formation.

purification of the protein from *E. coli.* The only cysteine residue in ECAD12 is the cysteine at position nine, which is not conserved among the classical cadherins. It is located at the end of the βA-strand in the ECAD1 domain that faces an opposite βA-strand in a second ECAD12 molecule (*10*), thus rendering intermolecular disulfide bond formation possible.

No noncovalent dimers were observed at the protein concentration used here.

ECAD1 and ECAD5, which were purified under reducing conditions and subsequently reoxidized, are monomeric in solution as revealed by a single band on nondenaturing gels (Figure 2C,D). Molar masses determined by sedimentation equilibrium experiments are close to the theoretical derived molar mass of the monomers (Table 1). The slightly decreased mobility of reduced and alkylated ECAD5 together with the absence of dimers under oxidizing conditions (Figure 2D) suggest intramolecular disulfide bond formation for ECAD5.

Sedimentation Equilibrium Experiments at High Protein Concentration. In order to study if ECAD12 is able to self-associate at concentrations similar to the high local concentrations of clustered E-cadherin molecules on the cell surface, we performed sedimentation equilibrium experiments at protein concentrations up to 0.45 mM (11 mg/mL). Sedimentation equilibrium centrifugation at high protein concentrations was carried out using the Yphantis short column method with Schlieren optics (*33*).

The weight average molar mass increased from 24 kD at a protein concentration of 0.02 mM to about 42 kD at 0.23 mM (Figure 3). The decrease of the molar mass at protein concentrations higher than 0.25 mM is due to a nonideality term observed in such experiments as described elsewhere (*30*). Assuming a monomer−dimer equilibrium, the best fit of the data by eqs 5 and 6 (see Experimental Procedures) resulted in K_d of 0.08 ± 0.02 mM (2 ± 0.5 mg of monomer/mL). In the absence of Ca^{2+}, ECAD12 does not self-associate (Figure 3).

Calcium Binding Monitored by Electrophoretic Mobility and Circular Dichroism Spectroscopy. Both oxidized and reduced ECAD12 showed an increase in electrophoretic mobility upon Ca^{2+} depletion in nondenaturing gel electrophoresis (Figure 2A). In contrast to that, no changes were

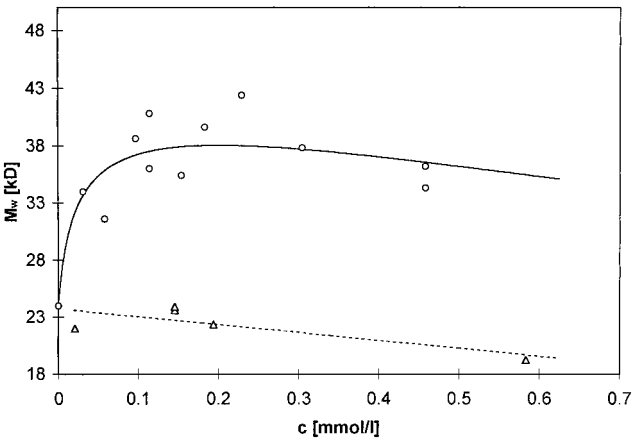

FIGURE 3: Self-association of ECAD12 monitored by sedimentation equilibrium experiments at high protein concentration. The change of the molar masses in dependence of the total monomer concentration at 2 mM Ca^{2+} is shown (○). The solid curve represents the best fit of the data resulting in a K_d of 0.8 ± 0.2 mM (2 ± 0.5 mg of monomer/mL). In the absence of Ca^{2+} no self-association was observed (△, dashed line).

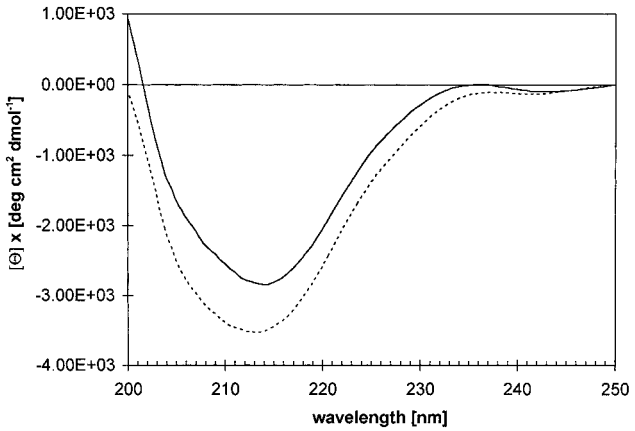

FIGURE 4: Circular dichroism spectra of the E-cadherin fragment ECAD12. The spectra of the calcium depleted (dashed line) and the calcium saturated (2 mM $CaCl_2$, solid line) recombinant E-cadherin fragment ECAD12 were recorded in a 2 mm quartz cell at a protein concentration of 6 μM in 20 mM Tris/HCl, pH 7.4, at 22 °C.

observed for the domains ECAD1, ECAD2, and ECAD5 (Figure 2C,D).

The mobility changes of ECAD12 suggest calcium induced conformational changes which were further studied by CD spectroscopy. Spectra of all fragments were very similar to the spectrum of the whole extracellular E-cadherin region with β-sheet structures as the main secondary structural element (*15*). Adding 2 mM Ca^{2+} to a Ca^{2+}-depleted sample of ECAD12 resulted in a significant increase of the mean molar residue ellipticity (Figure 4), whereas the spectra of the single domains did not change (data not shown). This clearly demonstrates that only ECAD12 is able to bind calcium ions and that its conformation is sensitive to calcium binding.

The calcium-dependent change of the CD signal was used as a signal for titration. The spectra were normalized, and the relative changes of the mean molar residue ellipticities at four different wavelengths were plotted against the total Ca^{2+} concentration. At the low protein concentration used in this experiment (6 μM), the total Ca^{2+} concentration can be set equal to the free Ca^{2+} concentration. The best fit of

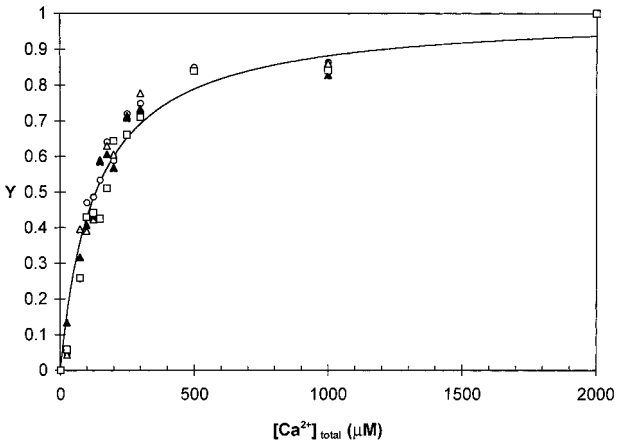

FIGURE 5: Calcium binding to a recombinant fragment consisting of the first two extracellular domains of E-cadherin (ECAD12) as monitored by circular dichroism. The fraction Y of the total change of the mean molar residue ellipticity at 210, 215, 220, and 230 nm is plotted against the total Ca^{2+} concentration. A dissociation constant of 360 μM and a Hill coefficient of 1 is obtained from the best fit to the experimental data.

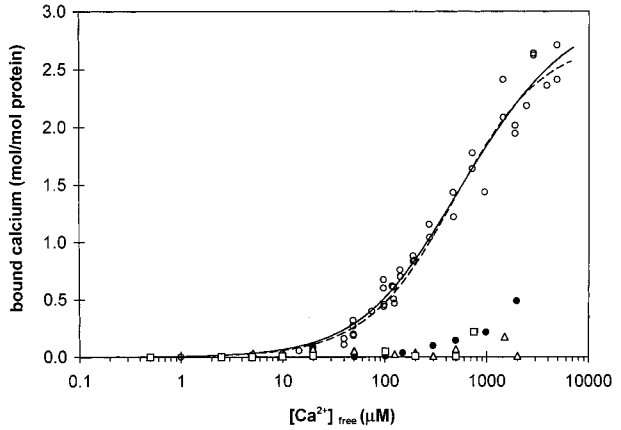

FIGURE 6: Calcium binding to a recombinant fragment consisting of the first two extracellular domains of E-cadherin (○) and to the single domain fragments ECAD1 (△), ECAD2 (●), and ECAD5 (□). The calcium-binding data were obtained by equilibrium dialysis using calcium concentrations up to 5 mM. The solid line represents the best fit to the data for ECAD12 using a model of ligand binding to three different classes of binding sites. This fit yields two K_d values of 330 μM and one K_d of 2000 μM. The dashed line represents the best fit to the data for ECAD12 using a model of one class of binding sites which results in 2.8 mol of bound Ca^{2+} per mol of protein and an average K_d of 460 μM. The data for the other fragments were not fitted (see Results).

the data using the Hill equation resulted in a parabolic curve with a midpoint at the total Ca^{2+} concentration of 360 μM (Figure 5) and a Hill coefficient equal to 1. Reversibility of the Ca^{2+}-induced increase of the CD signal was demonstrated by the addition of EDTA. Addition of Mg^{2+} (5 mM) to divalent ion-depleted ECAD12 had no effect on the CD signal.

Calcium Binding Monitored by Equilibrium Dialysis. Calcium binding to ECAD12 and to the 84 kD fragment was analyzed in more detail by equilibrium dialysis (Figures 6 and 7). The binding parameters were evaluated by fitting the data using a model of three different binding sites with different affinities or using the simplest model of ligand binding to a single class of binding sites. In all experiments, addition of Mg^{2+} (10 mM) had only minor effects on the stoichiometry of calcium binding (data not shown).

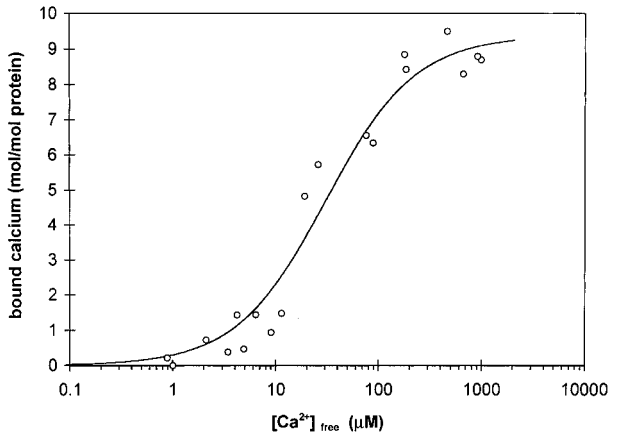

FIGURE 7: Calcium binding to a recombinant fragment consisting of the entire extracellular region of E-cadherin (84 kD fragment). The calcium-binding data were obtained by equilibrium dialysis. The line represents the best fit to these data using a model of ligand binding to a single class of binding sites. The fit resulted in nine mols of bound Ca^{2+} per mol of protein and an average K_d of 30 μM.

At high free Ca^{2+} concentrations (5 mM), 3 mol of Ca^{2+} is bound/mol of protein. The fit yielded two calcium-binding sites with a K_d of 330 μM and a third binding site with a much higher K_d of 2000 μM (Figure 6). The same goodness of fit with only little lower significance values (X^2 and R_{xy}) was obtained using a model with only one class of binding sites. This fit resulted in an average K_d of 460 μM for the three bound calcium ions (Figure 6). No significant calcium binding was observed for the single domain fragments. Only ECAD2 possesses calcium-binding affinity but to much lower extent than ECAD12 (Figure 6).

In order to compare the binding properties of ECAD12 with those of the entire extracellular region of E-cadherin we purified the so-called 84 kD fragment, expressed in a mammalian cell system, as described before (*11*). Equilibrium dialysis revealed that the 84 kD fragment, which consists of five domains with four putative Ca^{2+} binding pockets in between, binds approximately 9 mol of Ca^{2+}/mol of protein (Figure 7). Interestingly, the 84 kD fragment is already Ca^{2+} saturated at a free Ca^{2+} concentration of 1 mM. Using a model for a single class of binding sites, we obtained a K_d of 30 μM as an average value for these nine binding sites.

DISCUSSION

The observation that cadherin molecules cluster on the cell surface led to the model that high local concentrations are required for binding (*18*, *35*, *36*). Nevertheless, it has not been possible for a long time to prove homoassociation of cadherins in in vitro assays. Hence, extracellular regions of E-cadherin were artificially cross-linked by recombinantly fusing them to a pentameric coiled-coil domain at the C-terminus in order to mimick the clustering (*11*). Homoassociation of the pentamerized protein was demonstrated by ELISA type assays, and the local concentrations obtained by this approach were estimated to about 0.1−0.4 mM. Electron microscopy visualized that a large fraction of the E-cadherin strands within a pentamer associate by their N-terminal parts to dimers and that only these so-called strand dimers are able to interact with a second dimer formed in another pentamer. On the basis of these observations, a

cooperative two-step mechanism for the homoassociation has been proposed, in which a cadherin dimer emerging from one cell interacts with another dimer from the opposite cell, resulting in a tetrameric complex.

In the present work, we were able to detect about 50% dimer formation at a concentration of 0.08 mM of ECAD12, which is in good agreement with the data obtained by Tomschy et al. (*11*). The thus determined high K_d of about 0.08 mM for homoassociation explains the lack of association of the extracellular region of E-cadherin (*11*, *15*) and ECAD12 (present work) at 10 times lower concentrations. In contrast to Tomschy et al. (*11*), we were not able to detect formation of tetramers. This is most likely due to the fact that a possible monomer−dimer−tetramer equilibrium instead of a solely monomer−dimer equilibrium is much more difficult to resolve in a concentration range in which virial coefficients of all species play a dominant role.

Dimer formation of ECAD12 is strictly calcium dependent. The finding that the domain pair ECAD12 binds three calcium ions is in excellent agreement with the recently published X-ray structure of a similar fragment by Nagar et al. (*8*). The structure was solved for crystals which were grown in 5−10 mM $CaCl_2$ and revealed the binding of three calcium ions, designated as Ca1, Ca2, and Ca3 by the authors. The aspartate and glutamate rich binding motifs were, in part, already identified before (*12*, *13*, *37*), but only structural data showed that Ca^{2+} ions are bound in the interface between the domains. This is most clearly demonstrated in the structure of the domain pair in which Ca2 and Ca3 are bound both by residues located in domains 1 and 2, therefore being bridged by calcium-binding motifs of two consecutive domains. The location of calcium-binding sites in a so-called binding-pocket between two domains has been already proposed on the basis of the NMR and X-ray structure of single cadherin domains (*8*, *9*). In the X-ray structure of the N-terminal domain of N-cadherin (*9*), Ca^{2+} did not bind, but coordination of Yb^{3+} and UO_2^{2+} by an apparently incomplete calcium-binding site was observed.

Our results confirm that single domains 1 and 5 are not able to bind significant amounts of Ca^{2+} and only weak binding for a single calcium ion was observed for domain 2. We were also demonstrating that calcium binding to ECAD12 leads to a large, reversible conformational change reflected by changes in circular dichroism and electrophoretic mobility. We cannot judge if the observed conformational changes are only due to calcium binding in the linker region or if there are also induced changes apart from the binding site. Overduin et al. (*8*), however, describe calcium induced conformational changes which are transmitted to the adhesive interface in the N-terminal domain. Clearly, the binding of Ca^{2+} to the interface of the two domains rigidifies the otherwise flexible loop region (*10*). This also explains the large conformational change of the entire extracellular region as observed by electron microscopy (*15*).

Equilibrium dialysis experiments enabled us not only to determine number but also dissociation constants of bound Ca^{2+} ions. When fitting the data to a model with three sites of different affinities, least-squares analysis resulted in two sites with an identical K_d of 330 μM and a third low-affinity site with a K_d of 2 mM. This model can be nicely correlated with the Ca^{2+} coordination seen in the X-ray structure (*10*). It should be mentioned, however, that also a model with three equal binding sites (K_d = 460 μM), which represents the model with the least assumptions, yields a reasonable fit of only little lower significance values. We propose that Ca1 in the X-ray structure exhibits the low-affinity binding, since this Ca^{2+} is also coordinated by two water molecules and since all amino acid residues involved in coordinating Ca1 are also present in our ECAD1, which does not bind Ca^{2+}. The linker region at the C-terminus of ECAD1 is probably very flexible, leading to diminished binding; nevertheless, we would expect at least some binding affinities for this fragment if Ca1 would represent one of the higher affinity sites in ECAD12.

The extracellular region of E-cadherin contains four junctions between its five domains as putative Ca^{2+} binding pockets. By extrapolating the results for ECAD12, a total of 12 calcium-binding sites are predicted, but only nine were found by equilibrium dialysis. This indicates that not all the Ca^{2+} binding pockets are identical and that in some of the domain junctions with their rather variable binding motifs (*12*) less than three Ca^{2+} ions are bound. Equilibrium dialysis does not provide sufficient resolution for a determination of nine individual dissociation constants. It is, however, remarkable that the average K_d is an order of magnitude lower than the K_d of the higher affinity sites in ECAD12. This may indicate that the majority of the other sites in the extracellular region binds Ca^{2+} stronger than the sites in ECAD12. In addition, a positive cooperativity between the different sites in the entire extracellular part cannot be excluded, even if it cannot be deduced from our data. We are planning to express additional E-cadherin domain pairs in order to determine individual binding constants and numbers of binding sites for the remaining binding pockets. These data will either confirm or refute the existence of cooperativity between the different binding sites.

Calcium binding to the extracellular region of E-cadherin is substantial for its adhesive function and for the protection of the protein against protease digestion. This has been demonstrated in many classical studies (*12*, *15*, *16*, *38*, *39*). Recently, it has also been reported that the concentration of E-cadherin in adherens junctions requires a Ca^{2+} concentration of 1 mM (*40*). From this and earlier studies (*16*), a free Ca^{2+} concentration of about 10 (*16*)−30 μM (*40*) seems to be sufficient to protect E-cadherin against proteolytic degradation, but proper functioning of E-cadherin requires higher free Ca^{2+} concentrations.

The free Ca^{2+} concentration in the human blood is stringently regulated to 1.2 mM (*41*). Therefore, the Ca^{2+} concentration in other extracellular fluids was thought to be invariant, too. But there are also examples for variations in the extracellular Ca^{2+} concentration by a factor of about 10 that point to a possible role of Ca^{2+} as an extracellular messenger (*42*, *43*). The relatively high K_d values we determined for the Ca^{2+} binding to ECAD12 (0.3 and 2 mM) come under the range of possible calcium concentration changes. Besides, the N-terminal cadherin domain pair is probably the most important part of molecule for adhesion. This follows from mutational analysis (*17*), from total inhibition of E-cadherin mediated cell adhesion by point mutations in the calcium-binding region of ECAD12 (*13*), and from the restriction of contacts between two cadherins to the N-terminal part of the molecules (*11*). Therefore, a Ca^{2+} induced regulation of adhesiveness might be possible

by depletion and saturation of the calcium-binding sites in this domain pair.

The importance of the domain pair ECAD12 has been further substantiated by the recent finding that it is essential for the heterophilic interaction with αEβ7 (*44*). Remarkably, the heterophilic interaction with the integrin was abrogated by a single amino acid substitution in domain 1, and it was abrogated exclusively by this one, thus indicating that the binding site resides there. Moreover, mutants in which domains 1 or 2 were deleted proved to be ineffective for the adhesion to αEβ7 expressing cells, whereas mutants in which domains 3 or 4 were deleted showed the same adhesion activity as the wild-type extracellular fragment comprising all five domains. This data suggests that the calcium binding pocket between domains one and two is essential for the interaction with αEβ7 and that it cannot be replaced by any other of the four calcium binding pockets. Therefore, both homophilic and heterophilic interactions of E-cadherin depend on proper calcium binding between domains 1 and 2.

ACKNOWLEDGMENT

We thank Dr. Patrik Maurer for reading the manuscript and fruitful discussions, Prof. Dr. Rolf Kemler and Dr. Jörg Stappert for providing mouse E-cadherin cDNA, Dr. Paul Jenö for microsequencing and amino acid analysis, and Dr. Mark Eberhard for providing the EDTA-agarose column. We thank Charlotte Fauser and Ruth Landwehr for purifying the 84 kD fragment.

REFERENCES

1. Ranscht, B. (1994) *Curr. Opin. Cell Biol. 6*, 740−746.
2. Kemler, R., and Ozawa, M. (1989) *Bioassays 11*, 88−91.
3. Takeichi, M. (1995) *Curr. Opin. Cell Biol. 7*, 619−627.
4. Takeichi, M. (1991) *Science 251*, 1451−1455.
5. Gumbiner, B. M. (1996) *Cell 84*, 345−357.
6. Cepek, K. L., Shaw, S. K., Parker, C. M., Russel, J. G., Morrow, J. S., Rimm, D. L., and Brenner, M. B. (1995) *Nature 372*, 190−193.
7. Karecla, P. I., Bowden, S. J., Green, S. J., and Kilshaw, P. J.(1995) *Eur. J. Immunol. 25*, 852−856.
8. Overduin, M., Harvey, T. S., Bagby, S., Tong, K. I., Yau, P., Takeichi, M., and Ikura, M. (1995) *Science 267*, 386−389.
9. Shapiro, L., Fannon, A. M., Kwong, P. D., Thompson, A., Lehmann, M. S., Grübel, G., Legrand, J.-F., Als-Niesen, J., Colman, D. R., and Hendrickson, W. A. (1995) *Nature 374*, 327−337.
10. Nagar, B., Overduin, M., Ikura, M., and Rini, J. M. (1996) *Nature 380*, 360−364.
11. Tomschy, A., Fauser, C., Landwehr, R., and Engel, J. (1996) *EMBO J. 15*, 3507−3514.
12. Ringwald, M., Schuh, R., Vestweber, D., Eistetter, H., Lottspeich, F., Engel, J., Dölz, R., Jähnig, F., Epplen, J., Mayer, S., Müller, C., and Kemler, R. (1987) *EMBO J. 6*, 3647−3653.
13. Ozawa, M., Engel, J., and Kemler, R. (1990a) *Cell 63*, 1033−1038.
14. Becker, K.-F., Atkinson, M. J., Reich, U., Becker, I., Nekarda, H., Siewert, J. R., and Höfler, H. (1994) *Cancer Res. 54*, 3845−3852.
15. Pokutta, S., Herrenknecht, K., Kemler, R., and Engel, J. (1994) *Eur. J. Biochem. 223*, 1019−1026.
16. Hyafil, F., Babinet, C., Jakob, C. (1981) *Cell 26*, 447−454.
17. Nose, A., Tsuji, K., and Tackeichi, M. (1988) *Cell 54*, 993−1001.
18. Ozawa, M., Baribault, H., and Kemler, R. (1989) *EMBO J. 8*, 1711−1717.
19. Sanger, F., Nicklen, S., and Coulson, A. R. (1977) *Proc. Natl. Acad. Sci. 74*, 5463−5467.
20. Studier, F. W., and Moffatt, B.-A. (1986) *J. Mol. Biol. 189*, 113−130.
21. Herrenknecht, K. (1992) Ph.D. Dissertation, pp 51, Albert-Ludwigs-Universität, Freiburg im Breisgan, Germany.
22. Schägger, H., and von Jagow, G. (1987) *Anal. Biochem. 166*, 368−379.
23. Mach, H., Middaugh, C. R., and Lewis, R. V. (1992) *Anal. Biochem. 200*, 74−80.
24. Laemmli, U. K. (1970) *Nature 227*, 680−685.
25. Hunter, I., Schulthess, T., Bruch, M., Beck, K., and Engel, J. (1990) *Eur. J. Biochem. 188*, 205−211.
26. Jaenicke, R., and Rudolph, R. (1989) in *Protein Structure, a practical approach* (Creighton, T. E., Ed.) pp 191−223, IRL Press, Eynsham, Oxford, U.K.
27. Schachman, H. K. (1968) in *Biochemistry*, 3rd ed., Academic Press Inc., London, U.K.
28. Van Holde, K. E. (1985) in *Physical Biochemistry*, 2nd ed., pp 110−137, Prentice-Hall, Inc., Englewood Cliffs, NJ.
29. Yphantis, D. A. (1960) *Ann. NY Acad. Sci. 88*, 586−601.
30. Adams, E. T., Jr. (1965) *Biochemistry 4*, 1646−1645.
31. Eberhard, M., and Erne, P. (1991) *Eur. J. Biochem. 220*, 1333−1338.
32. Englund, P. T., Hubermann, J. A., Jovin, T. M., and Kronberg, A. (1969) *J. Biol. Chem. 244*, 3038−3044.
33. Zhao, Y., Pokutta, S., Maurer, P., Lindt, M., Franklin, R. M., and Kappes, B. (1994) *Biochemistry 33*, 3714−3721.
34. Ozawa, M., and Kemler, R. (1990b) *J. Cell Biol. 111*, 1645−1650.
35. Nagafuchi, A., and Takeichi, M. (1988) *EMBO J. 7*, 3679−3684.
36. McNeill, H., Ryan, T. A., Smith, S. J., and Nelson, W. J. (1993) *J. Cell Biol. 5*, 1217−1226.
37. Hatta, K., Nose, A., Nagafuchi, A., and Tackeichi, M. (1988) *J. Cell Biol. 106*, 873−881.
38. Takeichi, M. (1977) *J. Cell Biol. 75*, 464−474.
39. Gallin, W. J., Edelman, G. M., Cunningham, B. A. (1983) *Proc. Natl. Acad. Sci. U.S.A. 80*, 1038−1042.
40. Lewis, J. E., Jensen, P. J., Johnson, K. R., and Wheelock, M. J. (1995) *J. Cell Sci. 108*, 3615−3621.
41. Galyani, M., Ikrenyi, C., Fekrete, J., Ikrenyi, K., and Kovach, G. B. (1988) *Am. J. Physiol. 24*, F513-F519.
42. Brown, E. M., Vassilev, P. M., and Herbert, S. C. (1995) *Cell 83*, 679−682.
43. Maurer, P., Hohenester, E., and Engel, J. (1996) *Curr. Opin. Cell Biol. 8*, 609−617.
44. Karecla, P. I., Green, S. J., Bowden, S. J., Coadwell, J., and Kilshaw, P. J. (1996) *J. Biol. Chem. 271*, 30909−30915.

BI9705624